ISSN 0020-1685, Inorganic Materials, 2008, Vol. 44, No. 11, pp. 1183–1186. © Pleiades Publishing, Ltd., 2008.
Original Russian Text © Ya.I. Jafarov, N.A. Rzaeva, M.B. Babanly, 2008, published in Neorganicheskie Materialy, 2008, Vol. 44, No. 11, pp. 1314–1318.

Phase Equilibria in the Tl_2S–Tl_2Te–Tl_9BiTe_6–$TlBiS_2$ System[1]

Ya. I. Jafarov, N. A. Rzaeva, and M. B. Babanly
Baku State University, ul. Khalilova 23, Baku, AZ1148 Azerbaijan
e-mail: Babanly_mb@rambler.ru
Received September 14, 2007

Abstract—The phase equilibria in the Tl_2S–Tl_2Te–Tl_9BiTe_6–$TlBiS_2$ system have been studied by differential thermal analysis and x-ray diffraction. The results have been used to construct the *T–x* phase diagram along the Tl_2S–Tl_9BiTe_6 ($[TlBi_{0.333}S_{0.5}Te_{0.5}]$) and $TlBiS_2$–$Tl_2Te(Tl_9BiTe_6)$ joins, the 500-K section of the phase diagram of the Tl_2S–Tl_2Te–Tl_9BiTe_6–$TlBiS_2$ system, and its liquidus diagram. The invariant and univariant phase equilibria involved have been identified. The system has been shown to contain wide regions of Tl_2Te- and Tl_9BiTe_6-based quaternary solid solutions.

DOI: 10.1134/S002016850811006X

INTRODUCTION

There is considerable interest in multicomponent systems based on chalcogenides of heavy *p*-metals, motivated by the ongoing search for new thermoelectric materials [1–3].

Earlier, our group studied several quaternary systems based on thallium, antimony, and bismuth chalcogenides [4, 5]. Here, we report our findings on the phase equilibria in the reciprocal system $3Tl_2S + Bi_2Te_3 \rightleftharpoons 3Tl_2Te + Bi_2S_3$ in the composition region Tl_2S–Tl_2Te–Tl_9BiTe_6–$TlBiS_2$ (A).

The constituent chalcogenides of system A are semiconductors. In particular, Tl_2S has attractive photoelectric properties [6], and Tl_9BiTe_6 offers high thermoelectric performance. The electrical resistivity of Tl_9BiTe_6 is an order of magnitude higher than that of advanced thermoelectric materials. Its low thermal conductivity in comparison with other thermoelectric materials insures a high thermoelectric figure of merit [7].

Three of the four constituent binaries of system A—the pseudobinary joins Tl_2S–Tl_2Te ($TlBiS_2$) and Tl_2Te–Tl_9BiTe_6—were studied in [8–10]. The Tl_2S–Tl_2Te system [8] is pseudobinary, with a eutectic phase diagram and limited solid-solution series. The Tl_2S–$TlBiS_2$ system [9] contains an incongruently melting (820 K) compound of composition $Tl_4Bi_2S_5$. Tl_2Te and Tl_9BiTe_6 form a continuous series of solid solutions, which undergo a morphotropic phase transition at ≃20 mol % Tl_9BiTe_6 [10] .

[1] Presented in part at the XII Conference *High-Purity Substances and Materials: Preparation, Analysis, and Application*, Nizhni Novgorod, Russia, May 28–31, 2007.)

EXPERIMENTAL

For phase-equilibrium studies of system A, we synthesized Tl_2S, Tl_2Te, $TlBiS_2$, $Tl_4Bi_2S_5$, and Tl_9BiTe_6 by melting high-purity (99.999 wt %) elements in silica ampules pumped down to ~10^{-2} Pa. To obtain phase-pure $Tl_4Bi_2S_5$, the material was homogenized by annealing at 800 K for 200 h. The completion of reactions was checked by differential thermal analysis (DTA) and x-ray diffraction (XRD). The results were compared to earlier data [8–10].

Alloys of system A were synthesized along the Tl_2S–Tl_9BiTe_6 ($[TlBi_{0.333}S_{0.5}Te_{0.5}]$), Tl_2Te–$TlBiS_2(Tl_4Bi_2S_5)$, and $TlBiS_2$–Tl_9BiTe_6 joins. In addition, we synthesized several alloys with compositions off these joins. The alloys were prepared by melting appropriate mixtures of constituent chalcogenides in silica ampules sealed off under a vacuum of ~10^{-2} Pa and were then equilibrated by annealing 20–30 K below the solidus for ≃600 h. The annealing temperature was determined from DTA data for unannealed cast alloys.

The alloys were characterized by DTA (NTR-70 pyrometer, Chromel–Alumel thermocouples) and powder XRD (DRON-3 diffractometer, CuK_α radiation).

RESULTS AND DISCUSSION

Our results are presented in Figs. 1–3 and Tables 1 and 2. For the convenience of comparison, we use the same designations in the liquidus surface and sections of the *T–x–y* phase diagram in Figs. 1–3. Moreover, the *T–x–y* phase diagrams are presented with molar ratios of the constituent phases that enable comparison with the data in Figs. 2 and 3 without scaling the alloy compositions.

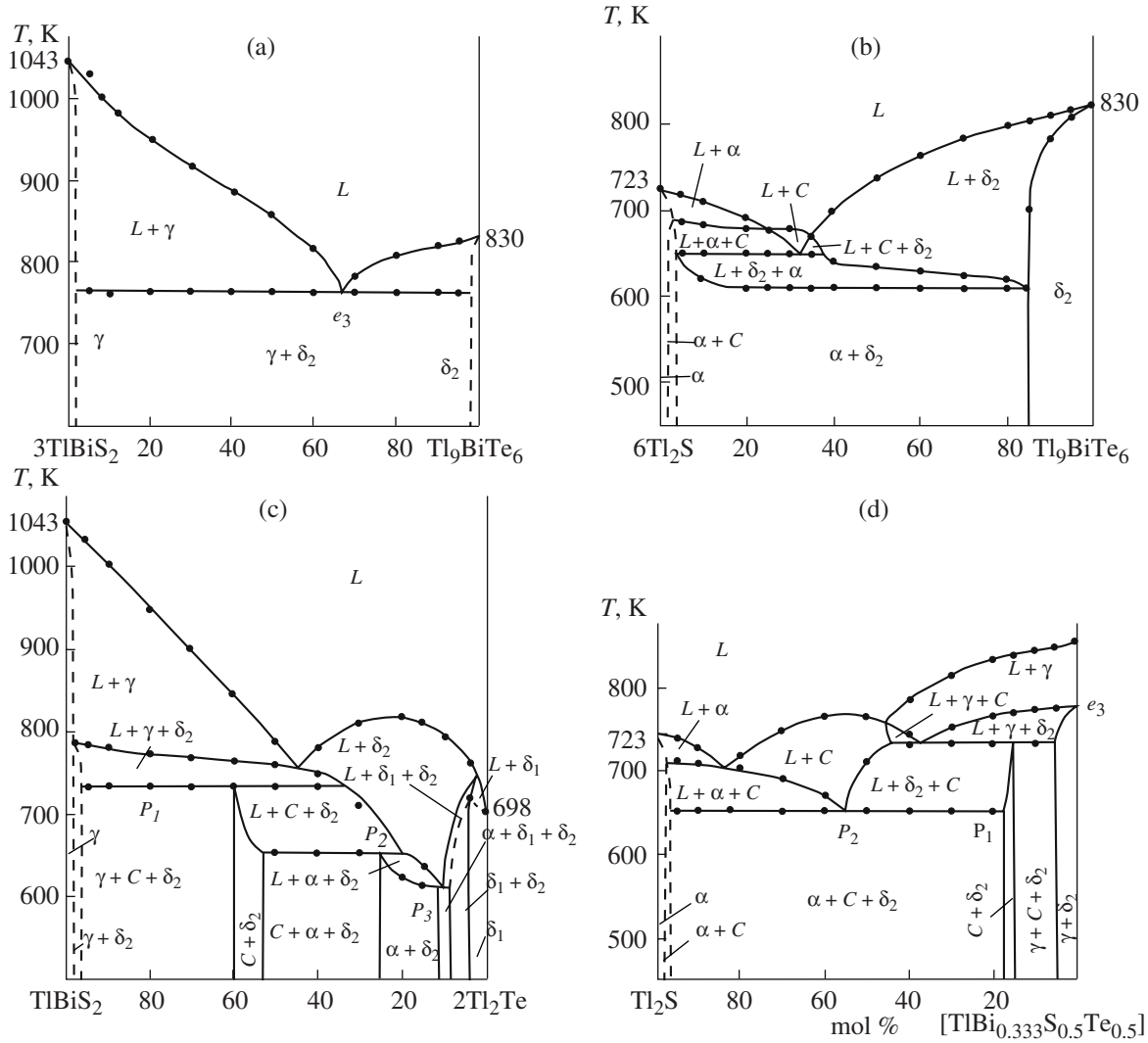

Fig. 1. Phase diagrams along the (a) $TlBiS_2$– Tl_9BiTe_6, (b) Tl_2S–Tl_9BiTe_6, (c) $TlBiS_2$–Tl_2Te, and (d) Tl_2S– $[TlBi_{0.333}S_{0.5}Te_{0.5}]$ joins of system A.

The $Tl_4Bi_2S_5$–$Tl_2Te(Tl_9BiTe_6)$ phase diagrams are not presented. The phase relations along these joins can easily be understood from the data in Figs. 2 and 3 and Tables 1 and 2.

The $TlBiS_2$–Tl_9BiTe_6 join (Fig. 1a) is almost pseudobinary, with a eutectic phase diagram (e_3) (the coordinates of the invariant and univariant equilibria involved are listed in Tables 1 and 2). The extent of the terminal solid solutions is ≃1–2 mol %.

The Tl_2S–Tl_9BiTe_6 join (Fig. 1b) is not pseudobinary, with complex phase relations. Its liquidus comprises three branches, corresponding to the primary crystallization of the α-, C- ($Tl_4Bi_2S_5$), and δ_2-phases (α and δ_2 are Tl_2S- and Tl_9BiTe_6-based solid solutions). Below the two-phase fields, univariant eutectic reactions (Table 2, curves e_2P_2, P_1P_2, P_2P_3) bring the system into a three-phase state: $L + \alpha + C$, $L + C + \delta_2$, and $L + \delta_2 + \alpha$. The horizontal representing the invariant peritectic reaction (Table 1, P_2) extends from ≃2 to ≃38 mol % Tl_9BiTe_6. In the composition range ≃2–85 mol % Tl_9BiTe_6, crystallization reaches completion through a univariant eutectic reaction (Table 2, P_2P_3), resulting in a two-phase equilibrium: $\alpha + \delta_2$.

The $TlBiS_2$–Tl_2Te join (Fig. 1c) is also not pseudobinary, with two-phase ($\gamma + \delta_2$, $C + \delta_2$, $\alpha + \delta_2$, $\delta_1 + \delta_2$) and three-phase ($\gamma + C + \delta_2$, $C + \alpha + \delta_2$, $\alpha + \delta_1 + \delta_2$) solid-state equilibria (γ and δ_1 are $TlBiS_2$- and Tl_2Te-based solid solutions). Its liquidus comprises three branches, corresponding to the primary crystallization of the γ-, δ_2-, and δ_1-phases. Below the liquidus are curves representing univariant eutectic ($L \rightleftarrows \gamma + \delta_2$, $L \rightleftarrows C + \delta_2$, $L \rightleftarrows \alpha + \delta_2$) and peritectic ($L + \delta_2 \rightleftarrows \delta_1$) reactions (Table 2). These reactions result in three-phase regions: $L + \gamma + \delta_2$, $L + C + \delta_2$, $L + \alpha + \delta_2$, and

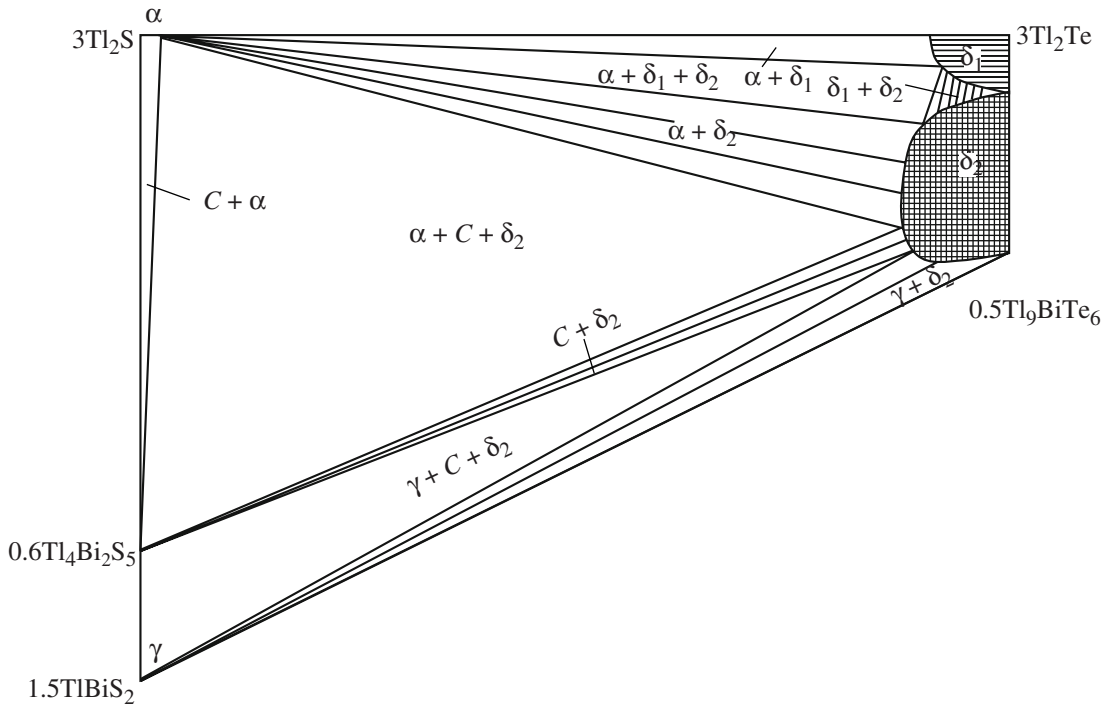

Fig. 2. 500-K section of the phase diagram of system A.

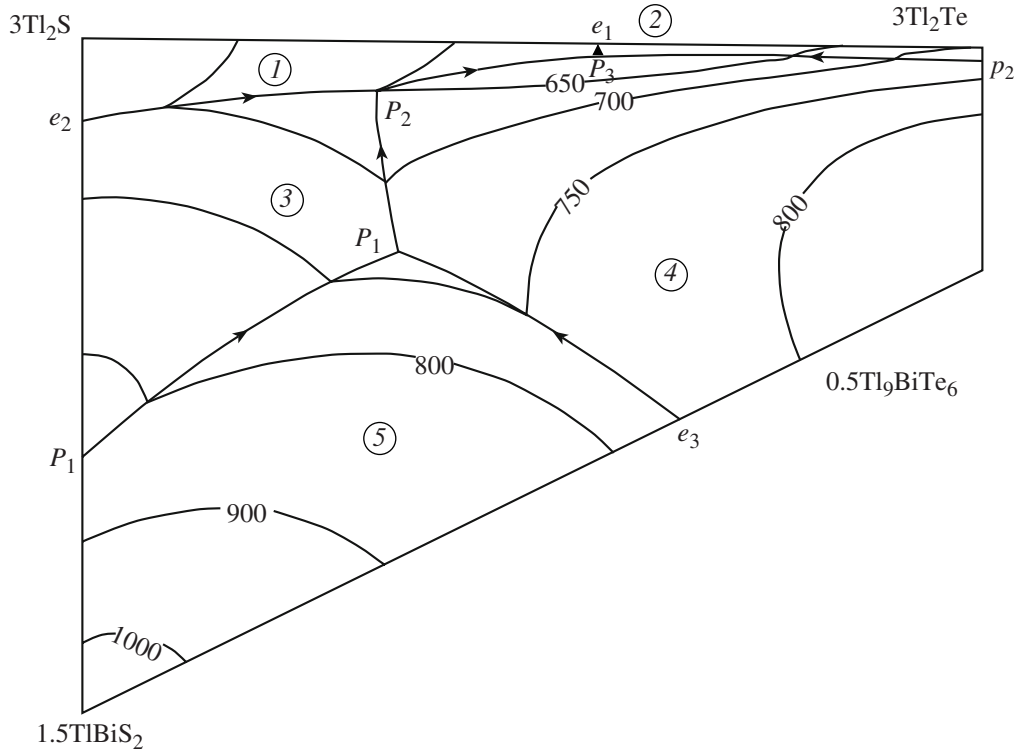

Fig. 3. Liquidus diagram of system A. Primary crystallization fields: (*1*) α, (*2*) δ_1, (*3*) *C*, (*4*) δ_2, (*5*) γ.

Table 1. Invariant equilibria in system A

Point in Fig. 3	Equilibrium	mol %			T, K
		$2Tl_2S$	$2Tl_2Te$	$TlBiS_2$	
e_1	$L \rightleftharpoons \alpha + \delta_1$	42	58	–	608
e_2	$L \rightleftharpoons \alpha + C$	88	–	12	713
e_3	$L \rightleftharpoons \gamma + \delta_2$	–	–	33	770
p_1	$L + \gamma \rightleftharpoons C$	38	–	62	815
p_2	$L + \delta_2 \rightleftharpoons \delta_1$	–	97	3	715
P_1	$L + \gamma \rightleftharpoons C + \delta_2$	53	22	25	730
P_2	$L + C \rightleftharpoons \alpha + \delta_2$	64	31	5	650
P_3	$L + \delta_2 \rightleftharpoons \delta_1 + \alpha$	41	56	3	610

$L + \delta_1 + \delta_2$, respectively. Crystallization reaches completion through univariant reactions (p_2P_3, P_2P_3, P_1P_2, and e_3P_1) in the composition ranges 5–9, 12–26, 52–59, and 98–99 mol % $TlBiS_2$ and through invariant reactions (P_3, P_2, and P_1) in the ranges 9–12, 26–52, and 59–98 mol % $TlBiS_2$ (Tables 1, 2).

The Tl_2S–[$TlBi_{0.333}S_{0.5}Te_{0.5}$] join (Fig. 1d) is also not pseudobinary, with a variety of heterogeneous equilibria, which can easily be understood by comparing Fig. 1d with Figs. 2 and 3.

Figure 2 shows the 500-K section of the phase diagram of system A, which clearly illustrates the subsolidus phase relations in this system. The α-phase field extends along the Tl_2S–Tl_2Te pseudobinary join and is ≃2 mol % in width and 5 mol % in length. The fields of the δ_1- and δ_2-phases (Tl_2Te- and Tl_9BiTe_6-based solid solutions, respectively) extend up to ≃12 mol %. $Tl_4Bi_2S_5$ dissolves insignificant amounts of other components. The homogeneity range of the γ-phase is ≃2 mol % in width. The system contains six two-phase regions ($\alpha + \delta_1$, $\delta_1 + \delta_2$, $\alpha + \delta_2$, $C + \alpha$, $C + \delta_2$, $\gamma + \delta_2$) and three three-phase regions ($\alpha + \delta_1 + \delta_2$, $C + \alpha + \delta_2$, $\gamma + C + \delta_2$). Note that the Tl_2Te–Tl_9BiTe_6 constituent binary has a morphotropic phase transition, $\delta_1 \rightleftharpoons \delta_2$, and the $\delta_1 + \delta_2$ two-phase region is essentially degenerate. Away from this binary system, the $\delta_1 + \delta_2$ region broadens, up to 5–6 mol % (Fig. 2).

The liquidus diagram (Fig. 3) comprises five primary crystallization fields, bounded by curves and points representing uni- and invariant equilibria (Tables 1, 2).

Table 2. Univariant equilibria in system A

Curve in Fig. 3	Equilibrium	Temperature range, K
$e_2 P_2$	$L \rightleftharpoons \alpha + C$	713–650
$p_1 P_1$	$L + \gamma \rightleftharpoons C$	815–730
$e_3 P_1$	$L \rightleftharpoons \gamma + \delta_2$	770–730
$p_2 P_3$	$L + \delta_2 \rightleftharpoons \delta_1$	715–610
$P_1 P_2$	$L \rightleftharpoons C + \delta_2$	730–650
$P_2 P_3$	$L \rightleftharpoons \alpha + \delta_2$	650–610
$P_3 e_1$	$L \rightleftharpoons \alpha + \delta_1$	610–608

REFERENCES

1. Kanatzidis, M.G., Role of Solid State Chemistry in the Discovery of New Thermoelectric Materials, *Semicond. Semimet.*, 2001, vol. 69, pp. 51–98.
2. Ioffe, A.F., *Poluprovodnikovye termoelementy* (Semiconductor Thermoelements), Moscow: Akad. Nauk SSSR, 1960.
3. Shelimova, L.E., Konstantinov, P.P., Karpinskii, O.G., et al., Thermoelectric Properties of $PbBi_4Te_7$-Based Anion-Substituted Layered Solid Solutions, *Neorg. Mater.*, 2004, vol. 40, no. 11, pp. 1307–1313 [*Inorg. Mater.* (Engl. Transl.), vol. 40, no. 11, pp. 1146–1152].
4. Jafarov, Ya.I., Mirzoeva, A.M., and Babanly, M.B., Reciprocal System $3Tl_2S + Bi_2Se_3 \rightleftharpoons 3Tl_2Te + Bi_2S_3$, *Zh. Neorg. Khim.*, 2006, vol. 51, no. 5, pp. 871–875.
5. Jafarov, Ya.I., Mirzoeva, A.M., Shikhiev, Yu.M., and Babanly, M.B., Reciprocal System $3TlSbS_2 + 2Sb_2Se_3 \rightleftharpoons 3TlSbSe_2 + 2Sb_2S_3$, *Az. Khim. Zh.*, 2006, no. 2, pp. 161–165.
6. Ashraf, I.M., Elshaiken, H.A., and Badr, A.M., Characteristics of Photoconductivity in Tl_2S Layered Single Crystals, *Phys. Status Solidi B*, 2004, vol. 241, no. 4, pp. 885–894.
7. Yamanaka Shinsuke, Kosuga Atsuko, and Kurosaki, K.J., Thermoelectric Properties of Tl_9BiTe_6, *J. Alloys Compd.*, 2003, vol. 352, no. 4. pp. 885–894.
8. Asadov, M.M., Babanly, M.B., and Kuliev, A.A., Phase Equilibria in the Systems Tl_2S–Tl_2Se and Tl_2S–Tl_2Te, *Izv. Akad. Nauk SSSR, Neorg. Mater.*, 1977, vol. 13, no. 8, pp. 1520–1521.
9. Babanly, M.B., Kesamanly, M.F., and Kuliev, A.A., System Tl–Tl_2S–Bi_2S_3–Bi, *Zh. Neorg. Khim.*, 1988, vol. 33, no. 9, pp. 2371–2375.
10. Babanly, M.B., Akhmad'yar, A., and Kuliev, A.A., System Tl_2Te–Bi_2Te_3–Te, *Zh. Neorg. Khim.*, 1985, vol. 30, no. 9, pp. 2356–2361.